

# A Comparative Study of Structural, Acidic and Hydrophilic Properties of Sn–BEA with Ti–BEA Using Periodic Density Functional Theory

Sharan Shetty,<sup>†,‡</sup> Bhakti S. Kulkarni,<sup>‡</sup> Dilip G. Kanhere,<sup>†</sup> Annick Goursot,<sup>§</sup> and Sourav Pal<sup>\*,‡</sup>

Centre for Modeling and Simulation, Department of Physics, University of Pune, Pune 411007, India, National Chemical Laboratory, Pune 411008, India, and Ecole de Chimie, Montpellier, Cedex 5, France

Received: October 9, 2007; In Final Form: December 20, 2007

Periodic density functional theory has been employed to characterize the differences in the structural, Lewis acidic and hydrophilic properties of Sn–BEA and Ti–BEA. We show that the incorporation of Sn increases the Lewis acidity of BEA compared to the incorporation of Ti. Hence, the present work gives insight into the role of Sn in increasing the efficiency of the oxidation reactions. The results also justify that the percentage of Sn substituted in BEA is less than Ti. The structural analysis shows that the first coordination shell of Sn is larger than that of Ti. However, the second coordination of both sites remains the same. The water adsorption properties of these substituted zeolites are quantified. Moreover, we explain the higher Lewis acidity of Sn than the Ti site on the basis of the Fukui functions and charge population analysis.

## 1. Introduction

Zeolite beta (BEA) has been used as one of the active catalysts for carrying out several organic reactions such as epoxidation of olefins,<sup>1</sup> aromatic and aliphatic alkylation,<sup>2</sup> acid-catalyzed reactions,<sup>3</sup> etc. Some of the important reactions which can be catalyzed by BEA include the Baeyer–Villiger oxidation (BVO) reaction and the Meerwein–Ponndorf–Verley reduction of aldehydes and Oppenauer's oxidation of alcohols (MPVO) reaction.<sup>4</sup> The reasons for using BEA as an efficient catalyst are its relatively large pore size, its flexible framework and its high acidity.<sup>5</sup> It has been well-established that the acidity of BEA can be finely tuned by the incorporation of various atoms such as B, Al, Ti, Zr, Fe, etc.<sup>6–9</sup> These sites substituted in the BEA framework act as active Bronsted or Lewis acid sites depending upon their valence states.<sup>8</sup> Among these atoms, Ti substitution in a BEA framework has proven to be an active catalyst for the epoxidation of olefins in the presence of H<sub>2</sub>O<sub>2</sub>.<sup>7,10</sup> The other Ti zeolites, which have been successfully used for the oxidation of small organic molecules, are the titanium silicalites (TS-1, TS-2).<sup>11</sup> Several studies have been reported to understand the differences of the activity and selectivity between these two zeolites.<sup>1,12</sup> Corma et al. have shown that these differences are due to the hydrophilic/hydrophobic nature of the Ti sites.<sup>19</sup> They showed that the Ti sites in TS are more hydrophobic than the Al–Ti–BEA. Hence, TS was preferred over Al–Ti–BEA when the solvent used in the reaction was prepared in an aqueous medium.

One of the challenges in this field is to increase the efficiency of a zeolite by substitution with other elements. Such an attempt has been made recently by incorporating Sn in BEA. Mal and Ramaswamy successfully synthesized the Al-free Sn–BEA.<sup>13</sup> In an interesting experimental work, Corma et al. showed that the incorporation of Sn in the BEA framework results in a more efficient catalyst for the BVO reaction in the presence of H<sub>2</sub>O<sub>2</sub>.<sup>14</sup>

In their study, a new mechanism was proposed for the oxidation of ketones. They showed that the Sn site in BEA activates the carbonyl group of the cyclohexanone followed by the attack of H<sub>2</sub>O<sub>2</sub>, unlike the Ti sites which initially activate the H<sub>2</sub>O<sub>2</sub>. This result was attributed to the higher Lewis acidity of the Sn site with respect to the Ti site. Hence, incorporation of Sn in BEA leads to a high selectivity toward the formation of lactones in the BVO reaction.<sup>14,15</sup> On this background, highly selective MPVO reactions were carried out more efficiently with Sn–BEA than Ti–BEA.<sup>16</sup> In these studies, it was shown that the Sn site is situated within the framework and no extraframework Sn was detected. Although much of the experimental studies have focused on the efficiency of the Sn–BEA, the higher Lewis acidity of the Sn site compared to the Ti site in BEA is still not known. Recently, Sever and Root used the M(OH)<sub>4</sub> (M = Sn, Ti) cluster models to investigate the reaction pathways for the BVO reaction.<sup>17</sup>

One of the important issues concerning the activity and selectivity of the zeolite is its hydrophobic/hydrophilic nature.<sup>18,19</sup> It is known that, if the zeolite is hydrophilic in nature, the water present in the solvent poisons the active sites. This hinders the kinetics of the reaction and decreases the activity of the zeolite. Corma et al. have bypassed this problem by modifying the catalyst design, which allows the use of Sn–BEA in the presence of aqueous media.<sup>20</sup> Very recently, Boronat et al. have done theoretical calculations using a Sn(OSiH<sub>3</sub>)<sub>3</sub>OH cluster model to understand the effect of H<sub>2</sub>O during the BVO reaction.<sup>31</sup> Their results show that one water molecule is permanently attached to the Sn active site. Interestingly, Fois et al. have studied the interaction of water molecules with the Ti sites in Ti–offretite using Car–Parrinello molecular dynamics.<sup>21</sup> They found that, at higher loading of water molecules, the Ti atom expands its coordination number.

In the past decade, several experimental and theoretical studies have been employed to characterize the role of Ti sites at a microscopic level in various Ti–zeolite systems.<sup>1,7,22–26</sup> It has been revealed that due to the high crystallinity, low Ti content and large quadrupolar moment of Ti, accurate information on the Ti sites in BEA is not possible through experimental

\* Corresponding author. E-mail: s.pal@ncl.res.in.

<sup>†</sup> University of Pune.

<sup>‡</sup> National Chemical Laboratory.

<sup>§</sup> Ecole de Chimie.

techniques.<sup>25</sup> Hence, it is necessary to use theoretical methods to explore the local behavior for, e.g., structure, electronic and bonding properties of these sites. Sastre and Corma have used *ab initio* calculations to discuss the role of the Ti sites in Ti-BEA and TS-1.<sup>26</sup> The energies of the lowest unoccupied molecular orbital (LUMO) of Ti-BEA and TS-1 with one Ti substituted in turn at every T site were shown to be different. Furthermore, the Ti sites in Ti-BEA were found to be more acidic than those in TS-1 and this acidity varies among all of the Ti sites in both zeolites.<sup>26</sup> This proves that not only do different Ti-containing zeolites have different acidities, but also different T sites within a particular zeolite would have varying acidities. Boronat et al. have also characterized the acidic characteristics of several transition metals substituted in BEA on the basis of LUMO energies.<sup>27</sup> Very recently, Bare et al. have used the EXAFS technique to investigate the Sn site in Sn-BEA.<sup>28</sup> They showed that Sn was not randomly distributed in BEA, and takes specific crystallographic sites, i.e., T5/T6 sites in their nomenclature, which corresponds to T1 and T2 in our nomenclature, following Newsam et al.<sup>29</sup> Surprisingly, they found that this substitution takes place through pairing of these sites, within the six-membered ring, i.e., two T1 or two T2. However, no explanation was given for this distribution. At the same time, in a theoretical work using a periodic approach based on density functional theory (DFT), we characterized the Sn sites in BEA.<sup>30</sup> We showed that the T2 site would be the most probable site for the Sn substitution based on thermodynamics consideration. Moreover, we found that the substitution of two Sn atoms per unit cell was thermodynamically unfavorable. This was consistent with the earlier experimental results.

As it can be seen from the above description, the incorporation of Sn in BEA proves to be a better catalytic site than Ti. Hence, detailed information on the differences in the properties of Sn and Ti sites in BEA, such as the quantification of the Lewis acidity, number of T atoms to be substituted in the unit cell and hydrophobicity, is of fundamental importance and is still to be resolved. The aim of the present theoretical study is to bring out the differences in these substituted BEA zeolites by analyzing their structural, electronic and water adsorption properties. Moreover, we use the local reactivity descriptors such as the Fukui functions (FFs) and charge population to analyze the Lewis acidic strength of Sn and Ti sites.

## 2. Methodology and Computational Details

Several theoretical studies based on a classical as well as quantum potential have been proposed to study the properties of zeolites.<sup>26,33–40</sup> It has been a practice to adopt cluster models cut from the zeolite crystals to study these properties. One of the obvious reasons to use the cluster model is that it is computationally cheap. Sauer et al. have conducted an extensive study of zeolites using cluster models.<sup>35,36</sup> A periodic approach provides a more realistic description to study the properties of a crystal.<sup>39,24</sup> Although zeolite catalysts are neither crystals nor periodic solids, it is more convenient to use periodic boundary conditions, when there are very few substituted sites per unit cell.

Earlier experimental studies have indeed proved that Sn and Ti sites in BEA are very few, that they are situated within the framework and during the BVO or MPVO reaction these sites do not dissociate from the framework.<sup>4a,15</sup> In the present work, we have employed the periodic DFT to investigate the properties of Sn-BEA and Ti-BEA. The advantage of using periodic boundary conditions is that the long range electrostatic interactions are included within Ewald summations. The unit cell of

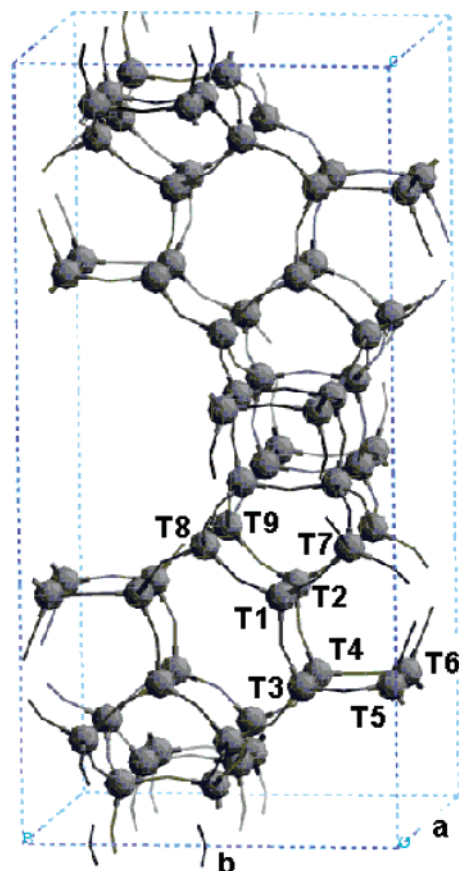


**Figure 1.** Crystallographically defined 9 T sites of BEA. The gray spheres represent the Si sites.

BEA is shown in Figure 1. The instantaneous stationary electronic ground state is calculated by solving the Kohn–Sham equation based on DFT. The valence electrons have been represented by the plane waves in conjunction with the Vanderbilt’s ultrasoft pseudopotential for the core.<sup>41</sup> It is worth mentioning that during the interaction between two systems the complete plane wave avoids the basis set superposition error. The exchange-correlation functional is expressed by the generalized gradient approximation (GGA) with the Perdew–Wang 91 functional.<sup>42</sup> The calculations were restricted to the gamma point in the Brillouin zone sampling. The energy cutoff used for the plane waves was 21.83 Ry (300 eV). The interaction between the water molecule and the Sn and Ti sites in BEA was studied using an energy cutoff of 36.74 Ry (500 eV).

For large systems, such as the present study, our study is limited to 36.74 Ry cutoff and our calculations may not have converged with respect to the energy cutoff. A much higher energy cutoff value has been used for the description of hydrogen bonding in the context of plane waves for HF clusters<sup>43</sup> using standard norm conserving pseudopotentials. On the other hand, we have used ultrasoft pseudopotentials, which may require a much lower energy cutoff. Further, our calculation is on a true periodic system, which may require much less cutoff than the free HF molecules enclosed in a box of 15 Å as in the work on HF clusters. For periodic systems, such as zeolites, cutoffs similar to the ones employed in the present study have been used<sup>44</sup> in earlier studies by others. However, it would be interesting to investigate the convergence of the adsorption energies with energy cutoffs for systems studied in this paper in the future.

The energies corresponding to the HOMO, LUMO, and HOMO–LUMO gaps are obtained using the periodic calcula-

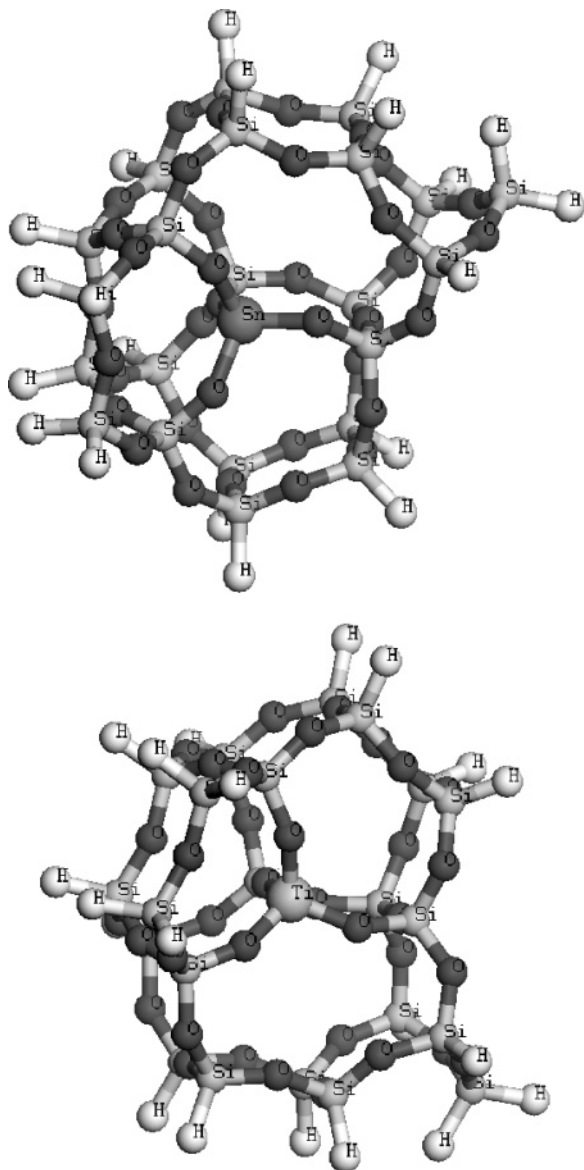


**Figure 2.** The cluster models cut from the optimized periodic Sn– and Ti–BEA systems. The T sites are T2 and T1 for the Sn– and Ti–BEA systems, respectively.

tions at all nine T sites of Sn– and Ti–BEA. The above calculations have been performed by the VASP code.<sup>45</sup> The charge population and local reactivity descriptors have been calculated using the cluster model, cut from the optimized periodic systems of Sn–BEA and Ti–BEA. The cluster model cuts are represented in Figure 2. The clusters have been cut considering the most reactive T sites, i.e., T2 and T1 for Sn– and Ti–BEA, respectively. The clusters have been terminated with the H atoms. These clusters were reoptimized by constraining the terminal H atoms and relaxing all of the other atomic positions. The cluster calculations have been carried out by the DFT approach and B3LYP functional with the basis set DZVP.<sup>46</sup> These calculations are done using the GAMESS program.<sup>50</sup>

BEA is a high silica zeolite and consists of two different ordered polytypic series, viz., polymorph A and polymorph B.<sup>29</sup> It has two mutually perpendicular straight channels with a cross section of  $0.76 \times 0.64$  nm which run along the *a* and *b* directions. Intersecting to these, at right angles, a helical channel of  $0.55 \times 0.55$  nm also exists along the *c*-axis. This gives rise to a three-dimensional pore system of 12-membered ring aperture. The unit cell of an ideal fully siliceous BEA consists

**TABLE 1: Optimized Structural Parameters of Sn–BEA. Average Sn–O Bond Lengths, Sn–O–Si Bond Angles and Sn–Si Distances of All the 9 T Sites of Sn–BEA**

T site	Sn–O (Å)	Sn–O–Si (deg)	Sn–Si (Å)
T1	1.911	143.5	3.336
T2	1.909	144.2	3.341
T3	1.910	140.6	3.241
T4	1.917	136.0	3.281
T5	1.913	142.2	3.297
T6	1.910	141.2	3.297
T7	1.911	140.6	3.282
T8	1.908	140.0	3.282
T9	1.912	137.8	3.270

**TABLE 2: Optimized Structural Parameters of Ti–BEA. Average Ti–O Bond Lengths, Ti–O–Si Bond Angles and Ti–Si Distances of All the 9 T Sites of Ti–BEA**

T site	Ti–O (Å)	Ti–O–Si (deg)	Ti–Si (Å)
T1	1.799	151.7	3.302
T2	1.797	152.4	3.304
T3	1.794	145.0	3.220
T4	1.797	145.4	3.233
T5	1.799	148.1	3.257
T6	1.799	148.5	3.263
T7	1.794	149.0	3.269
T8	1.795	147.4	3.249
T9	1.798	144.0	3.225

of 192 atoms with 64 Si and 128 O atoms distributed within the tetragonal lattice of dimensions of  $12.6 \times 12.6 \times 26.2$  Å. There are nine distinct crystallographically defined T sites, as shown in Figure 1. We adopt the experimental structure as defined by Newsam et al. and accordingly define the nine T sites in the unit cell of BEA.<sup>29</sup>

The structural optimization of the Si and Sn– and Ti–BEA has been carried out in two steps. In the first step, the conjugate gradient method was used to optimize the unit cell of BEA. The optimization was considered to be achieved when the maximum forces on the atoms were less than  $0.1$  eV/Å. In the second step, these optimized geometries were reoptimized with the quasi-Newton method unless the maximum force on the atoms was less than  $0.06$  eV/Å. One should note that during the optimization the cell shape of the unit cell has been fully relaxed, while keeping its volume constant. The reason is that the percentage of Sn and Ti in BEA is only 1/u.c. We expect that if the concentration of the Sn or Ti is increased in BEA the volume of the cell along with the shape has to be relaxed. In the case of Sn– and Ti–BEA, each of the nine distinct T sites were substituted by Sn and Ti atoms (i.e., Si/(Sn or Ti) = 63/1, respectively), and were optimized. Once the active site in Sn– and Ti–BEA was confirmed, one water molecule was introduced near these active sites and the same optimization procedure was followed as discussed above. The structural data for the Sn–BEA has been taken from a recent publication by us.<sup>30</sup>

### 3. Results and Discussion

**3.1. Structure of Sn–BEA and Ti–BEA.** We have already discussed the structure and energetics of Sn–BEA in a recent publication.<sup>30</sup> In the present work, we briefly recall this discussion which is necessary for comparing it with the structure and energetics of Ti–BEA and also to study the water adsorption property.

Tables 1 and 2 present the optimized structural details of all nine T sites of Sn–BEA and Ti–BEA, respectively. It should be noted that only the average bond distances and bond angles are presented. It can be seen from Table 1 that the Sn–O bond



distance ranges between 1.908 and 1.917 Å, the Sn–O–Si bond angle ranges from 136 to 144.2° and the Sn–Si distance is around  $3.241 \pm 0.100$  Å. Very recently, Bare et al., with the help of the EXAFS technique, showed that the Sn–O bond distances and Sn–Si distances in Sn–BEA were around 1.906 and 3.5 Å, respectively.<sup>28</sup> This clearly shows that the theoretical results presented by us are in good agreement with the experimental results. However, the theoretical results of Bare et al. were not consistent with their experimental data. This may be due to keeping the shape of the unit cell fixed during the optimization and using the local density approximation exchange-correlation potential in their study.<sup>28</sup> On the other hand, we have relaxed the lattice vectors of the unit cell during the optimization and also used the GGA exchange-correlation potential, as explained in the earlier section. The change in the local coordination of the T site in Sn–BEA compared to the Si–BEA has been illustrated in the earlier study.

Table 2 shows that the average Ti–O bond distances of the nine T sites in BEA vary from 1.794 to 1.799 Å. These values are in good agreement with the earlier works on Ti–BEA.<sup>7</sup> Compared to Sn–O bond distances, the Ti–O distances are smaller. This is due to the larger atomic size of Sn with respect to Ti. From the data of Tables 1 and 2, it can be noticed that the average Sn–O and Ti–O bond lengths are very similar for all T sites, whereas the corresponding bond angles have a large range of variation. Moreover, in both the Sn– and Ti–BEA models, the largest average angles belong to the T1 and T2 sites. The average experimental values of T1–O–T and T2–O–T angles in the unsubstituted Si–BEA are 155.3 and 155.9°, respectively, and they also correspond to the largest T–O–T angles in the framework. If we compare Sn and Ti substituted in the framework with Si, we get the expected order for average T–O bond lengths Sn–O > Ti–O > Si–O, with around 0.12–0.15 Å difference at each replacement. The average T1–O–T or T2–O–T bond angles vary as Sn–O–Si < Ti–O–Si < Si–O–Si.

These Ti–O–Si bond angles which range between 144 and 152° are larger than the Sn–O–Si bond angles with a range between 136.0–143.5°. Due to the angular flexibility, the Ti–Si distance differs only by  $\sim 0.04$  Å from the Sn–Si distance. Although the first coordination shell radius of Ti is smaller than that of Sn, the second coordination shells are at similar distances. The adaptation of the BEA framework to Sn and Ti substitution results thus in a quite localized deformation of the siliceous framework. Hence, we can infer that the difference in adsorption properties between Sn– and Ti–BEA should be mainly due to the electronic differences of these sites.

**3.2. Energetics of Sn–BEA and Ti–BEA.** In this subsection, we discuss the thermodynamic stability of Sn–BEA and Ti–BEA. This is done by calculating the cohesive energies for each of the nine T sites in Sn–BEA and Ti–BEA. Cohesive energy of a solid is defined as the difference between the energy of the bulk (solid) at equilibrium and the energy of the constituent atoms in their ground state.<sup>30</sup> Cohesive energy does not account for the kinetic formation of the system, neither for the different nature of the synthesis intermediates generated in aqueous solution, which can generate different routes for the solid growth.

The cohesive energies of all nine substituted T sites of Sn–BEA and Ti–BEA are given in Table 3. In our earlier investigation on the energetics of Sn–BEA, we showed that the substitution of Sn in the BEA framework decreases the cohesive energy.<sup>30</sup> Hence, the incorporation of Sn in BEA was shown to be thermodynamically less stable than the Si–BEA.

**TABLE 3: Cohesive Energies of All the 9 T Sites of Sn–BEA and Ti–BEA**

T site	cohesive energy (eV)	
	Sn–BEA	Ti–BEA
T1	–1521.387	–1530.797
T2	–1521.681	–1530.767
T3	–1521.468	–1530.210
T4	–1521.523	–1530.045
T5	–1521.405	–1530.014
T6	–1521.431	–1530.570
T7	–1521.457	–1530.359
T8	–1521.621	–1530.415
T9	–1521.323	–1530.282

On this basis, we explained the fact that the incorporation of Sn in the BEA framework is restricted. Interestingly, Bare et al. predicted the formation of Sn pairs as the active sites, where the two Sn atoms were shown to be on the opposite sides of a six-membered ring.<sup>28</sup> They showed that one of these pairs is present per 8 u.c. of BEA. Unfortunately, at present, it is out of scope to consider 8 u.c. of BEA. Nevertheless, we have carried out the calculations placing two Sn atoms per u.c. at the T1 and T2 (T5 and T6 according to Bare et al.) positions which are situated in the six-membered ring and are on the opposite side of each other (Figure 1). We found that this does not increase the cohesive energy.

The cohesive energy of Si–BEA is –1527.902 eV.<sup>30</sup> From Table 3, we see that the cohesive energy of Ti–BEA is about 3 eV higher than that of Si–BEA. This indicates that the incorporation of Ti in BEA is thermodynamically more favorable than that of Sn. Among the nine T sites of Ti–BEA, we found that the T1 and T2 sites have the highest stability, and that T5 is the least stable. We have also calculated the cohesive energy with two Ti per u.c. (i.e., Ti/Si = 2/62 per u.c.). The two Ti atoms were incorporated at two different T2 positions at a distance of 9 Å. This showed an increase in the cohesive energy of about 3 eV compared to one Ti per u.c. This reveals that more Ti could be incorporated in BEA than Sn. We want to stress that these calculations are carried out on a dehydrated solid resulting from a thermodynamically driven synthesis, ignoring the effects of the various ingredients and formation conditions, i.e., the nature and energies of the synthesis intermediates. Nevertheless, these results are consistent with the earlier experimental works, where it has been shown that the amount of incorporated Ti is larger than that of Sn in BEA.<sup>7,15</sup>

**3.3. Lewis Acidity of Sn–BEA and Ti–BEA.** Earlier experimental studies have conjectured that Sn acts as a better Lewis acidic site than Ti in BEA.<sup>14–16</sup> Hence, Sn–BEA acts as a more active catalyst for the oxidation reactions. This motivated us to compare the Lewis acidity of Sn– and Ti–BEA. First, one must recall that the Lewis acidity, being related with an electron acceptor character, can be correlated with the global electron affinity of the solid. Qualitatively, LUMO energies can be used for a comparison between the electron affinities of Sn– and Ti–BEA.<sup>26,27</sup> The HOMO and the LUMO energies, and their corresponding HOMO–LUMO gaps of Sn–BEA and Ti–BEA, have been reported in Table 4. Globally, the average LUMO energy among the Sn substituted models is lower than that for the Ti ones. In our earlier results on Sn–BEA, we have shown that out of the nine T sites the T1 and the T2 sites have low LUMO energies compared to the other T sites, and would be the probable sites for the reaction.<sup>30</sup> Interestingly, T1 and T2 have been proposed as the most probable sites for Sn substitution from EXAFS experiments.<sup>28</sup> The two corresponding LUMOs have similar low energies,

**TABLE 4: Energies of the HOMO, LUMO and HOMO–LUMO Gaps of the 9 T Sites of Sn–BEA and Ti–BEA**

T site	Sn–BEA			Ti–BEA		
	HOMO (eV)	LUMO (eV)	gap (eV)	HOMO (eV)	LUMO (eV)	gap (eV)
T1	−3.124	1.333	4.457	−3.135	1.417	4.552
T2	−3.125	1.366	4.491	−3.133	1.469	4.602
T3	−3.131	1.557	4.688	−3.121	1.548	4.669
T4	−3.117	1.421	4.538	−3.120	1.492	4.612
T5	−3.131	1.450	4.581	−3.152	1.500	4.652
T6	−3.120	1.426	4.546	−3.145	1.453	4.598
T7	−3.121	1.419	4.540	−3.156	1.486	4.642
T8	−3.117	1.497	4.614	−3.144	1.470	4.620
T9	−3.114	1.506	4.620	−3.121	1.454	4.575

**TABLE 5: Mulliken and Löwdin Charges of Sn and Ti Atoms in Their Respective Configurations**

T site	Mulliken	Löwdin
Sn	1.57	1.28
Ti	1.32	0.89

making these two models good candidates as Lewis acids.<sup>27</sup> Both sites have also the smallest HOMO–LUMO gap. A smaller gap, in a solid, correlates with a larger global softness. The most probable Sn–BEA solids would thus correspond to the most Lewis acidic and the more “soft” models.

In the case of Ti–BEA, we can see from Table 4 that the T1 site has the lowest LUMO energy, whereas T3 has the highest. We can also notice that T1 and T2, which have the largest cohesive energies, have also low HOMO–LUMO gaps, with T1 having the smallest. Considering these two factors together, we propose that these sites would also be the most favorable sites for the substitution by Ti and also for the reaction to take place. We propose thus that, in both cases, Sn and Ti would be more probably substituted at the T1 and T2 sites. Considering their LUMO energies, about 0.1 eV lower for Sn–BEA, we can infer that Sn–BEA is more Lewis acidic than Ti–BEA. Moreover, with the corresponding HOMO–LUMO gaps being lower for Sn–BEA than for Ti–BEA, this also suggests that Sn–BEA is a softer acid. This conclusion is also supported by the following trend: whereas the cohesive energies of the T1–T9 substituted Sn–BEA solids spreads on 0.36 eV, those of the Ti–BEA solids spread over 0.66 eV. Despite its smaller radius, Ti has thus less ability to adapt to the various geometric environments, showing the behavior of a “harder” species.

Local reactivity descriptors such as condensed electrophilic and nucleophilic FFs and charge populations have been used to interpret the acidic strength of the Sn and Ti sites.<sup>47–49</sup>

Table 5 describes the Mulliken and Löwdin charge populations. We can see from Table 5 that the positive charge on Sn is higher than that on Ti. This indicates that there is a charge buildup on the Ti compared to Sn. This probably arises due to the back-donation of electrons from the neighboring oxygen atoms to the empty d-orbitals of Ti, lowering its positive charge and therefore its Lewis acidity.

The values of electrophilic FFs ( $f^+$ ) and nucleophilic FFs ( $f^-$ ) obtained through the Löwdin population scheme are given in Table 6. The electrophilic ( $f_k^+$ ) and nucleophilic ( $f_k^-$ ) FFs of a particular  $k$ th atom are defined as

$$f_k^+ \approx q_k^{N_0+1} - q_k^{N_0}$$

$$f_k^- \approx q_k^{N_0} - q_k^{N_0-1}$$

**TABLE 6: Condensed Electrophilic ( $f^+$ ) and Nucleophilic ( $f^-$ ) FFs of the 9 T Sites of Sn–BEA and Ti–BEA**

atom	Sn–BEA		Ti–BEA	
	$f^+$	$f^-$	$f^+$	$f^-$
T = Sn/Ti	0.2465	0.00265	0.2170	0.0024
Si	0.0267	0.0015	0.0245	0.0011
Si	0.0308	0.0009	0.0258	0.0013
Si	0.0255	0.0031	0.0236	0.0028
Si	0.0250	0.0037	0.0241	0.0030
O	0.0465	0.0002	0.0737	0.0003
O	0.0464	0.0048	0.0677	0.0038
O	0.0461	0.0075	0.0705	0.0037
O	0.0408	0.00373	0.0714	0.0002

$q_k$  values are the electronic population of the  $k$ th atom of a particular species. It can be seen that the electrophilic FFs (Table 6) of Sn and Ti in their respective configurations are higher than those of the other atoms. This shows that the Sn and Ti sites act as the probable Lewis acidic sites for the nucleophilic attack. Interestingly, the Sn site is slightly more electrophilic than the Ti site. This clearly indicates the higher Lewis acidity of Sn compared to the Ti site.

**3.4. Hydrophilicity of Sn–BEA and Ti–BEA.** One of the important issues concerning the selectivity toward the organic molecules in zeolites is the hydrophobic/hydrophilic character of these catalysts.<sup>18</sup> Indeed, for reactions such as BVO and MPVO in the presence of aqueous solvents, zeolites containing both Lewis acidity and hydrophobicity would be the most appropriate.<sup>20,31</sup> In fact, being a product of reaction, water is always present in the catalyst pores. However, this presence is not desirable, because its adsorption is competitive with that of reactants and also due to the product hydrolysis. On a perfect silicalite surface, water is physisorbed, i.e., its interaction energy is weak, mainly due to van der Waals forces. As soon as defects are present, water may bind to the silanols or dissociate and react with the surface.<sup>32</sup> In order to be hydrophobic, zeolites must thus present less or no defects. If this is achieved, i.e., for highly hydrophobic samples, experimental results show that substituted Ti–BEA is much more hydrophobic than Sn–BEA.<sup>20</sup> Although it is difficult to compare Ti–BEA and Sn–BEA with a high loading of water, it is of particular interest to investigate, at the microscopic level, the coordination of Sn and Ti sites in the presence and absence of one water molecule. For this comparison, Sn and Ti have been located at sites T2 and T1, respectively. The full systems have then been optimized with an higher energy cutoff to account for the hydrogen bonding as mentioned in section 2.

Table 7 gives the averaged optimized T–O(BEA), T–OH<sub>2</sub> bond lengths, T–O–Si bond angles and T–Si distances, where T = Sn and Ti. We can see that after hydration, the Sn–O distance has been increased by 0.013 Å and the Sn–O–Si angle is also increased by about 3.2° with respect to the dehydrated Sn–BEA. The bond distance between the Sn site and the H<sub>2</sub>O is 2.38 Å. The hydrated Ti–BEA shows a similar trend with a Ti–O bond length and the Ti–O–Si bond angle which have been increased by 0.025 Å and 2.3°, respectively. The Ti–OH<sub>2</sub> bond distance is 2.44 Å. We see that the Sn–OH<sub>2</sub> distance is shorter than Ti–OH<sub>2</sub>. In order to understand the adsorption of the H<sub>2</sub>O molecule to the T sites, we have calculated the binding energy (BE) of a single water molecule to the Sn and Ti sites in BEA (Table 7). This is done as follows

$$BE = E_{\text{complex}}(\text{BEA} + \text{H}_2\text{O}) - \{E(\text{BEA}) + E(\text{H}_2\text{O})\}$$

**TABLE 7: Structural Parameters and Binding Energies (BEs) of Sn–BEA and Ti–BEA in the Presence of H<sub>2</sub>O**

	Sn–BEA + H <sub>2</sub> O	Ti–BEA + H <sub>2</sub> O
T–O(BEA) (Å)	1.924	1.822
T–O–Si (deg)	146.72	154.70
T–Si (Å)	3.38	3.34
T–OH <sub>2</sub> (Å)	2.38	2.44
BE (kJ/mol)	–32.07	–13.0

As can be seen from Table 7, the BEs of a water molecule to the Sn and Ti sites are –32.07 and –13.0 kJ/mol, respectively. This clearly shows that the water molecule has an exothermic interaction with the Sn and Ti sites. This has been confirmed experimentally for Ti–BEA zeolite.<sup>7</sup> Furthermore, the Ti–BEA and H<sub>2</sub>O complex is ~20 kJ/mol less stable than the Sn–BEA and H<sub>2</sub>O complex. This also confirms the Sn site in BEA has high Lewis acidity and is more hydrophilic compared to Ti–BEA.

It must be recalled that interaction energies calculated with DFT based methods do not include van der Waals attractive contributions. In recent work, these dispersion terms have been added empirically<sup>51</sup> or using adequate correlation functionals.<sup>52</sup> It is easy to give an a posteriori estimate of the van der Waals stabilization of water bound to the Sn or Ti sites in BEA, using an empirical correction. Using our optimized Sn and Ti structures, the van der Waals stabilization energy of the bound water molecule has been calculated using the universal force field.<sup>53</sup> The following energies have been found: –13.8 kJ/mol for Sn–BEA and –10 kJ/mol for Ti–BEA. Since these empirical van der Waals terms are additive, one can infer that a water dimer would form a very low exothermic complex with the Sn–BEA model but would still be nonbonding with the Ti model. Hence, these results show that Ti–BEA is less hydrophilic than Sn–BEA. This confirms the earlier experimental findings.<sup>20a</sup>

#### 4. Conclusions

The present theoretical investigation reveals the differences between the Sn–BEA and Ti–BEA based on their structural, Lewis acidic and hydrophilic properties. Our analysis shows that the Sn and Ti atoms may occupy T2 and/or T1 crystallographic positions in BEA. Although the first coordination shell of Sn is larger than Ti, the second coordination shell in both model zeolites is similar. This explains the relaxation of the local environment of the substituted site. The structural data on Sn–BEA and Ti–BEA presented in this work are in good agreement with the earlier experimental studies. The cohesive energy results demonstrate that the incorporation of Ti is more favorable than Sn in BEA. Nevertheless, we show that Sn–BEA is more Lewis acidic than Ti, and hence proves to be a more efficient catalyst for the oxidation reactions than Ti–BEA. Interestingly, we have used the local reactivity descriptors such as condensed electrophilic and nucleophilic FFs to explain the higher Lewis acidic strength of Sn than Ti. The charge population analysis quantifies the back-donation of the electrons in Ti which is not seen in Sn. One of the important aspects concerning the activity and selectivity of the zeolite which we have addressed in the present work, is the hydrophilic nature of the Sn and Ti sites in BEA. Our results show that Sn–BEA is more hydrophilic than Ti–BEA.

The present work gives insight into the microscopic properties of the active sites in Sn–BEA and Ti–BEA and the differences between them, which would have been otherwise difficult to understand through experimental methods.

**Acknowledgment.** We partially acknowledge the Indo-French Centre for Promotion of Advanced Research (IFCPAR) for funding and to the Center of Excellence in Scientific Computing at NCL.

#### References and Notes

- (1) Corma, A.; Esteve, P.; Martinez, A. *J. Catal.* **1996**, *161*, 11.
- (2) Bellussi, G.; Pazzuconi, G.; Perego, C.; Girotti, G.; Terzoni, G. *J. Catal.* **1995**, *157*, 227.
- (3) Creighton, E. J.; Ganeshie, S. D.; Downing, R. S.; van Bekkum, H. *J. Mol. Catal.* **1997**, *115*, 457.
- (4) (a) Jansen, J. C.; Creighton, E. J.; Njo, S. L.; van Koningsveld, H.; van Bekkum, H. *Catal. Today* **1997**, *38*, 205. (b) Kunkeler, P. J.; Zuurdeeg, B. J.; van der Waal, J. C.; van Bokhoven, J. A.; Koningsberger, D. C.; van Bekkum, H. *J. Catal.* **1998**, *180*, 234.
- (5) (a) Wadlinger, R. L.; Kerr, G. T.; Rosinski, E. J. U.S. Patent 3308069, 1967. (b) Tuan, V. A.; Li, S.; Noble, R. D.; Falconer, J. L. *Environ. Sci. Technol.* **2003**, *37*, 4007.
- (6) (a) Sen, T.; Chatterjee, M.; Sivasanker, S. **1995**, 207. (b) de Ménorval, L. C.; Buckermann, W.; Figueras, F.; Fajula, F. *J. Phys. Chem.* **1996**, *100*, 465. (c) Juttu, G. C.; Lobo, R. F. *Catal. Lett.* **1999**, *62*, 99. (d) Dimitrova, R.; Neinska, Y.; Mihályi, M.; Pal-Borbély, G.; Spassova, M. *Appl. Catal., A* **2004**, *266*, 123. (e) Pérez-Ramírez, J.; Groen, J. C.; Brückner, A.; Kumar, M. S.; Bentrup, U.; Debbagh, M. N.; Villacusa, L. A. *J. Catal.* **2005**, *232*, 318.
- (7) (a) Blasco, T.; Cambor, M. A.; Corma, A.; Pérez-Pariente, J. *Am. Chem. Soc.* **1993**, *115*, 11806. (b) van der Waal, J. C.; van Bekkum, H. *J. Mol. Catal.* **1997**, *124*, 137. (c) Carati, A.; Flego, C.; Massara, P.; Millini, R.; Carluccio, L.; Parker, W. O., Jr.; Bellussi, G. *Microporous Mesoporous Mater.* **1999**, *30*, 137.
- (8) van Santen, R. A.; Kramer, G. J. *Chem. Rev.* **1995**, *95*, 637.
- (9) Blasco, T.; Cambor, M. A.; Corma, A.; Esteve, P.; Guil, J. M.; Martinez, A.; Perdigón-Melón, J. A.; Valencia, S. *J. Phys. Chem. B* **1998**, *102*, 75.
- (10) (a) Saxton R. J.; Zajacek J. G.; Crocco G. L. *Zeolites* **1996**, *17*, 315. (b) Corma, A.; Domine, M. E.; Gaona, J. A.; Navarro, M. T.; Rey, F.; Valencia, S. *Stud. Surf. Sci. Catal.* **2001**, *135*, 1812.
- (11) (a) Taramasso, M.; Perego, G.; Notari, B. U.S. Patent 4,410,501, 1983. (b) Reddy, J. S.; Sivasanker, S. *Catal. Lett.* **1991**, *11*, 241. (c) Huybrechts, D. R. C.; De Bruycker, L.; Jacobs, P. A. *Nature* **1990**, *345*, 240.
- (12) (a) van der Waal, J. C.; Lin, P.; Rigutto, M. S.; van Bekkum, H. *Stud. Surf. Sci. Catal.* **1996**, *105B*, 1093. (b) Corma, A.; Cambor, M. A.; Esteve, P.; Martínez, A.; Pérez-Pariente, J. *J. Catal.* **1994**, *145*, 151.
- (13) Mal, N. K.; Ramaswamy, A. V. *Chem. Commun.* **1997**, 425.
- (14) Corma, A.; Nemeth, L. T.; Renz, M.; Valencia, S. *Nature* **2001**, *412*, 423.
- (15) Renz, M.; Blasco, T.; Corma, A.; Fornés, V.; Jensen, R.; Nemeth, L. *Chem.—Eur. J.* **2002**, *8*, 4708.
- (16) Corma, A.; Domine, M. E.; Nemeth, L.; Valencia, S. *J. Am. Chem. Soc.* **2002**, *124*, 3194.
- (17) (a) Sever, R. R.; Root, R. W. *J. Phys. Chem. B* **2003**, *107*, 10521. (b) Sever, R. R.; Root, R. W. *J. Phys. Chem. B* **2003**, *107*, 10848.
- (18) Corma, A. *J. Catal.* **2003**, *216*, 298.
- (19) Stelzer, J.; Paulus, M.; Hunger, M.; Weitkamp, J. *Microporous Mesoporous Mater.* **1998**, *22*, 1.
- (20) (a) Corma, A.; Domine, M. E.; Valencia, S. *J. Catal.* **2003**, *215*, 294. (b) Corma, A.; Renz, M. *Chem. Commun.* **2004**, 550. (c) Corma, A.; Fornés, V.; Iborra, S.; Mifsud, M.; Renz, M. *J. Catal.* **2004**, *221*, 67.
- (21) Fois, E.; Gamba, A.; Spanó, E. *J. Phys. Chem. B* **2004**, *108*, 154.
- (22) Zicovich-Wilson, C. M.; Dovesi, R.; Corma, A. *J. Phys. Chem. B* **1999**, *103*, 988.
- (23) (a) Pei, S.; Zajac, G.; Kaduk, J.; Faber, J.; Boyanov, B.; Duck, D.; Fazzini, D.; Morrison, Yang, D. *Catal. Lett.* **1993**, *21*, 333. (b) Lopez, A.; Tuilier, M.; Guth, J.; Delmotte, L.; Popa, J. *Solid State Chem.* **1993**, *102*, 480. (c) Scarano, D.; Zecchina, A.; Bordiga, S.; Geobaldo, F.; Spoto, G.; Petrini, G.; Leofanti, G.; Padovan, M.; Tozzola, G. *J. Chem. Soc., Faraday Trans.* **1993**, *89*, 4123. (d) Neurok, M.; Manzer, L. E. *J. Chem. Soc., Chem. Commun.* **1996**, 1133.
- (24) Zicovich-Wilson, C. M.; Dovesi, R. *J. Phys. Chem. B* **1998**, *102*, 1411.
- (25) (a) Notary, B. *Catal. Today* **1993**, *18*, 163. (b) Berger, S.; Bock, W.; Marth, C.; Raguse, B.; Reetz, M. *Magn. Reson. Chem.* **1990**, *28*, 559.
- (26) Sastre, G.; Corma, A. *Chem. Phys. Lett.* **1999**, *302*, 447.
- (27) Boronat, M.; Corma, A.; Renz, M.; Viruela, R. M. *Chem.—Eur. J.* **2006**, *12*, 7076.
- (28) Bare, S. R.; Kelly, S. D.; Sinkler, W.; Low, J. J.; Modica, F. S.; Valencia, S.; Corma, A.; Nemeth, L. T. *J. Am. Chem. Soc.* **2005**, *127*, 12924.
- (29) Newsam, J. M.; Treacy, M. M. J.; Koetsier, W. T.; de Gruyter, C. B. *Proc. R. Soc. London, Ser. A* **1988**, *420*, 375.
- (30) Shetty, S.; Pal, S.; Kanhere, D. G.; Goursot, A. *Chem.—Eur. J.* **2006**, *12*, 518.



- (31) Boronat, M.; Corma, A.; Renz, M.; Sastre, G.; Viruela, P. M. *Chem.—Eur. J.* **2005**, *11*, 6905.
- (32) (a) Ma, Y.; Foster, A. S.; Nieminen, R. M. *J. Chem. Phys.* **2005**, *122*, 144709. (b) Mischler, C.; Horbach, J.; Kob, W.; Binder, K. *J. Phys.: Condens. Matter* **2005**, *17*, 4005.
- (33) Jentys, A.; Catlow, C. *Catal. Lett.* **1993**, *22*, 251.
- (34) Neurok, M.; Manzer, L. E. *J. Chem. Soc., Chem. Commun.* **1996**, 1133.
- (35) de Man, A. J. M.; Sauer, J. *J. Phys. Chem.* **1996**, *100*, 5025.
- (36) Sauer, J. *Chem. Rev.* **1989**, *89*, 199.
- (37) Valerio, G.; Goursot, A.; Vetrivel, R.; Malkina, O.; Malkin, V.; Salahub, D. R. *J. Am. Chem. Soc.* **1998**, *120*, 11426.
- (38) Maurin, G.; Bell, R. G.; Devautour, S.; Henn, F.; Giuntini, J. C. *Phys. Chem. Chem. Phys.* **2004**, *6*, 182.
- (39) Nicholas, J. B.; Hess, A. C. *J. Am. Chem. Soc.* **1994**, *116*, 5428.
- (40) Rozanska, X.; Demuth, T.; Hutschka, F.; Hafner, J.; van Santen, R. A. *J. Phys. Chem. B* **2002**, *106*, 3248.
- (41) Vanderbilt, D. *Phys. Rev. B* **1990**, *41*, 7892.
- (42) Perdew, J. P.; Wang, Y. *Phys. Rev. B* **1992**, *45*, 13244.
- (43) Raynaud, C.; Maron, L.; Jolibois, F.; Daudey, J. P.; Esteves, P. M.; Ramírez-Solís, A. *Chem. Phys. Lett.* **2005**, *414*, 161.
- (44) (a) Vos, A. M.; Rozanska, X.; Schoonheydt, R. A.; van Santen, R. A.; Hutschka, F.; Hafner, J. *J. Am. Chem. Soc.* **2001**, *123*, 2799. (b) Termath, V.; Haase, F.; Sauer, J.; Hutter, J.; Parrinello, M. *J. Am. Chem. Soc.* **1998**, *120*, 8512. (c) Stich, I.; Gale, J. D.; Terakura, K.; Payne, M. C. *J. Am. Chem. Soc.* **1999**, *121*, 3292.
- (45) (a) Kresse, G.; Hafner, J. *Phys. Rev. B* **1994**, *49*, 14251. (b) Kresse, G.; Furthmüller, *Comput. Mater. Sci.* **1996**, *6*, 15.
- (46) Godbout, N.; Salahub, D. R.; Andzelm, J.; Wimmer, E. *Can. J. Chem.* **1992**, *70*, 560.
- (47) (a) Parr, R. G.; Yang, W. *J. Am. Chem. Soc.* **1984**, *106*, 4049. (b) Yang, Y.; Parr, R. G. *Proc. Natl. Acad. Sci. U.S.A.* **1985**, *82*, 6723.
- (48) Roy, R. K.; Krishnamuthy, S.; Geerlings, P.; Pal, S. *J. Phys. Chem. A* **1998**, *102*, 3746.
- (49) Roy, R. K.; Pal, S.; Hirao, K. *J. Chem. Phys.* **1999**, *110*, 8236.
- (50) Schmidt, M. W.; Baldrige, K. K.; Boatz, J. A.; Elbert, S. T.; Gordon, M. S.; Jensen, J. H.; Koseki, S.; Matsunga, N.; Nguyen, K. A.; Su, S.; Windus, T. L.; Dupuis, M.; Montgomery, J. A. *J. Comput. Chem.* **1993**, *14*, 1347.
- (51) (a) Wu, Q.; Yang, W. *J. Chem. Phys.* **2002**, *116*, 515. (b) Zimmerli, U.; Parrinello, M.; Koumoutsakos, P. *J. Chem. Phys.* **2004**, *120*, 2693. Grimme, S. *J. Comput. Chem.* **2004**, *25*, 1463.
- (52) Dion, M.; Rydberg, H.; Schröder, E.; Langreth, D. C.; Lundqvist, B. I. *Phys. Rev. Lett.* **2004**, *92*, 246401.
- (53) Rappe, A. K.; Casewit, C. J.; Colwell, K. S.; Goddard III, W. W.; Skiff, M. M. *J. Am. Chem. Soc.* **1992**, *114*, 10024.